Long-term effects of pulmonary endarterectomy on right ventricular stiffness and fibrosis in chronic thromboembolic pulmonary hypertension

Braams, N.J.; Kianzad, A.; Wezenbeek, J. van; Wessels, J.N.; Jansen, S.M.A.; Andersen, S.; ... ; Meijboom, L.J.

Circulation: Heart Failure

ORIGINAL ARTICLE

Long-Term Effects of Pulmonary Endarterectomy on Right Ventricular Stiffness and Fibrosis in Chronic Thromboembolic Pulmonary Hypertension

Natalia J. Braams, MD*; Azar Kianzad, MD*; Jessie van Wezenbeek, MSC; Jeroen N. Wessels, MD; Samara M.A. Jansen, MD; Stine Andersen, MD, PhD; Anco Boonstra, MD, PhD; Esther J. Nossent, MD; J. Tim Marcus, PhD; Ahmed A. Bayoumy, MD, PhD; Clarissa Becher, MSc; Marie-José Goumans, PhD; Asger Andersen, MD, PhD; Anton Vonk Noordegraaf, MD, PhD; Frances S. de Man, PhD; Harm Jan Bogaard, MD, PhD†; Lilian J. Meijboom, MD, PhD†

BACKGROUND: Surgical removal of thromboembolic material by pulmonary endarterectomy (PEA) leads within months to the improvement of right ventricular (RV) function in the majority of patients with chronic thromboembolic pulmonary hypertension. However, RV mass does not always normalize. It is unknown whether incomplete reversal of RV remodeling results from extracellular matrix expansion (diffuse interstitial fibrosis) or cellular hypertrophy, and whether residual RV remodeling relates to altered diastolic function.

METHODS: We prospectively included 25 patients with chronic thromboembolic pulmonary hypertension treated with PEA. Structured follow-up measurements were performed before, and 6 and 18 months after PEA. With single beat pressure-volume loop analyses, we determined RV end-systolic elastance (Ees), arterial elastance (Ea), RV–arterial coupling (Ees/Ea), and RV end-diastolic elastance (stiffness, Eed). The extracellular volume fraction of the RV free wall was measured by cardiac magnetic resonance imaging and used to separate the myocardium into cellular and matrix volume. Circulating collagen biomarkers were analyzed to determine the contribution of collagen metabolism.

RESULTS: RV mass significantly decreased from 43±15 to 27±11g/m^2 (−15.9 g/m^2 [95% CI, −21.4 to −10.5]; P<0.0001) 6 months after PEA but did not normalize (28±9 versus 22±6 g/m^2 in healthy controls [95% CI, 2.1 to 9.8]; P<0.01). On the contrary, Eed normalized after PEA. Extracellular volume fraction in the right ventricular free wall increased after PEA from 31.0±3.8 to 33.6±3.5% (3.6% [95% CI, 1.2–6.1]; P=0.013) as a result of a larger reduction in cellular volume than in matrix volume ($P_{interaction}$=0.0013). Levels of MMP-1 (matrix metalloproteinase-1), TIMP-1 (tissue inhibitor of metalloproteinase-1), and TGF-β (transforming growth factor-β) were elevated at baseline and remained elevated post-PEA.

CONCLUSIONS: Although cellular hypertrophy regresses and diastolic stiffness normalizes after PEA, a relative increase in extracellular volume remains. Incomplete regression of diffuse RV interstitial fibrosis after PEA is accompanied by elevated levels of circulating collagen biomarkers, suggestive of active collagen turnover.

Key Words: extracellular volume ■ magnetic resonance imaging ■ pulmonary hypertension ■ right ventricular function ■ vascular diseases ■ ventricular remodeling

Correspondence to: Harm Jan Bogaard, MD, PhD, Department of Pulmonary Medicine, Amsterdam UMC, Vrije Universiteit Amsterdam, De Boelelaan 1117, 1081 HV Amsterdam, the Netherlands. Email hj.bogaard@amsterdamumc.nl
*N.J. Braams and A. Kianzad contributed equally.
†H. Jan Bogaard and L.J. Meijboom contributed equally as last authors.
Supplemental Material is available at https://www.ahajournals.org/doi/suppl/10.1161/CIRCHEARTFAILURE.122.010336.
For Sources of Funding and Disclosures, see page 893.

Circulation: Heart Failure is available at www.ahajournals.org/journal/circheartfailure

WHAT IS NEW?

- The present study is the first longitudinal study assessing extracellular volume in the relatively thin-walled right ventricle (RV) before and after pulmonary endarterectomy (PEA) in chronic thromboembolic pulmonary hypertension.
- Extracellular volume in the RV free wall increases after PEA indicating residual RV fibrosis.
- Despite persistent fibrosis, RV diastolic stiffness normalizes after PEA.
- Circulating levels of collagen biomarkers are increased both pre- and post-surgery.

WHAT ARE THE CLINICAL IMPLICATIONS

- Although diffuse interstitial fibrosis regression is not complete in the RV and collagen synthesis biomarkers remained increased after PEA, they were not associated with increased RV diastolic stiffness.
- Further investigations are needed to assess the clinical implications of residual RV remodeling after PEA for chronic thromboembolic pulmonary hypertension.

Nonstandard Abbreviations and Acronyms

CMR	cardiac magnetic resonance
CTEPH	chronic thromboembolic pulmonary hypertension
ECV	extracellular volume fraction
LV	left ventricular
MMP-1	matrix metalloproteinase 1
mPAP	mean pulmonary artery pressure
PEA	pulmonary endareterectomy
PVR	pulmonary vascular resistance
RV	right ventricular
RVFW	right ventricular free wall
RVIP	RV interventricular insertion point
TGF-β	transforming growth factor-β
TIMP-1	tissue inhibitor of metalloproteinase-1

Chronic thromboembolic pulmonary hypertension (CTEPH) is characterized by persistent occlusion of the pulmonary arteries by organized thromboembolic material and remodeling of the pulmonary vasculature. Eventually, pulmonary vascular resistance (PVR) will increase leading to chronic right ventricular (RV) pressure overload.[1] The RV adapts to pressure overload by cellular hypertrophy. In advanced CTEPH, structural cardiac remodeling occurs by RV dilatation together with a decreased RV systolic and diastolic function, often accompanied by diffuse interstitial deposition of collagen (fibrosis).[2–5] Previous studies have shown that surgical removal of thromboembolic material by pulmonary endarterectomy (PEA) leads within months to hemodynamic improvement and reverse remodelling of the RV.[6] However, in the majority of patients RV mass does not normalize after surgery.[6–8] Comparable observations were done in chronic left ventricular (LV) pressure overload due to aortic stenosis, where surgical aortic valve replacement leads to a regression, but not normalization of LV mass.[9] In a recent study, extracellular volume fraction (ECV) mapping by cardiac magnetic resonance imaging (MRI) was used to demonstrate that a persistent increase in LV mass after aortic valve replacement is in part explained by persistent fibrosis, caused by a lesser reduction in extracellular matrix than in cellular hypertrophy after surgery.[10] Whether persistent fibrosis also explains the increased RV mass and is associated with increased diastolic stiffness after PEA for CTEPH is unknown.

ECV assessment by cardiac magnetic resonance (CMR) provides robust data on diffuse interstitial fibrosis that correlates well with histology and differentiates between cellular (myocytes, fibroblast, endothelial, red blood cells) and extracellular (extracellular matrix, blood plasma) compartments.[11–17] Data on myocardial ECV of the RV after PEA are lacking, as the relatively thin-walled RV after PEA complicates the differentiation between blood and myocardium required for ECV determination. Previous studies in patients with atrial fibrillation have shown that measuring T1 and calculating ECV at end-systole is feasible and reduces T1 variablity in CMR.[18,19]

Circulating collagen biomarkers are elevated in PAH and are associated with prognosis and disease progression.[20] However, whether levels of collagen metabolites are altered in CTEPH, and whether they reflect changes in the RV after surgery is unknown. We hypothesized that a persistently increased RV mass after PEA is in part explained by residual fibrosis and might consequently affect RV systolic and diastolic function. By combining structured assessment of RV hemodynamics, pressure-volume analyses to assess RV systolic function and diastolic stiffness, end-systolic ECV mapping of the right ventricular free wall (RVFW) and circulating biomarkers at baseline, 6 and 18 months after PEA, we aimed to investigate long-term reverse remodeling in patients with CTEPH.

METHODS

Study Subjects

In a prospective multicenter study, all adult patients diagnosed with CTEPH and treated with PEA are screened for inclusion in the tertiary referral centres for CTEPH in Amsterdam University Medical Center, The Netherlands and Aarhus University Hospital, Denmark (the 2A3C study). The current analysis is based on patients included between September 2017 and March 2020 in Amsterdam. CTEPH was diagnosed according to the most recent guidelines at the time of inclusion.[1] Exclusion criteria were (1) renal failure (glomerular

filtration rate below 30 mL/min per 1.73 m^2), (2) contraindications for cardiac MR such as metallic implants, known gadolinium intolerance, claustrophobia, (3) cognitive impairment preventing judgement concerning study participation. Residual PH was defined as a mean pulmonary artery pressure (mPAP) >20 mm Hg and PVR ≥240 dynes/s/cm^5 according to the revised hemodynamic definition proposed at the Sixth World Symposium on Pulmonary Hypertension.[21] Structured follow-up measurements were performed using CMR, blood analysis, and right heart catheterization before PEA and 6 and 18 months after surgery (Figure S1). For the assessment of diffuse interstitial fibrosis, CMR with T1 mapping was performed before and after intravenous contrast administration before PEA and 6 and 18 months after surgery. To determine circulating collagen biomarkers (see below), blood samples were collected at the same 3 time points. Single beat pressure-volume loop analysis was used to determine load-independent RV diastolic stiffness (Eed).[22] The study protocol was approved by the Medical Ethics Review Committee of the Amsterdam University Medical Center (2017.060) and written informed consent was obtained from each participant before study entry. The data that support the findings of this study are available from the corresponding author upon reasonable request.

Surgery

The PEA procedure has been described previously.[23,24] All patients were discussed in our expert multidisciplinary pulmonary hypertension (PH) team. Operability was based on accessibility of pulmonary artery obstructions, imbalance between increased PVR and amount of accessible occlusions suggesting microvascular disease and comorbidities. According to our center's clinical protocol, patients are not routinely subjected to imaging after PEA to assess residual peripheral clot burden.

Right Heart Catheterization and Pressure-Volume Loop Analysis

Hemodynamic assessment was performed using a fluid-filled balloon-tipped 7F Swan-Ganz catheter (131HF7, Baxter Healthcare Corp, Irvine, CA). During continuous electrocardiographic monitoring, mean right atrial pressure, mPAP, and pulmonary artery wedge pressure were recorded and mixed venous oxygen saturation (SvO2) was measured. Cardiac output was determined by thermodilution or direct Fick method. PVR (dynes/s per cm^5) was calculated as 80×(mPAP—pulmonary artery wedge pressure)/cardiac output.[25]

Pressure-Volume Loop Analysis

A detailed delineation of the load-independent RV PV loop analysis has been described previously.[25] The slope of the end-systolic pressure-volume relationship (Ees) was calculated as follows (Figure 1):

$$Ees = \frac{\text{Piso} - \text{RVESP}}{SV}$$

The maximal isovolumic pressure (Piso) was determined using the single-beat method of Sunagawa et al[26] as described previously.[25,27] In short, an inverted cosine wave was fitted over the RV pressure curve using the isovolumic contraction period (from end-diastole to the point of maximal rate of pressure rise

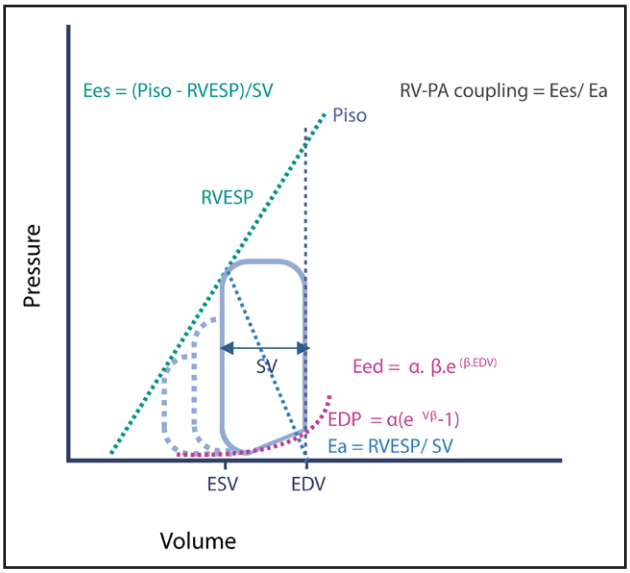

Figure 1. Schematic overview of pressure-volume relations of the right ventricle (RV).
Ees is the slope of the end-systolic pressure-volume relation as a measure of RV contractility, Ea is a measure of the arterial load and diastolic elastance, and Eed is ventricular elastance at end-diastole, determined as the slope of the diastolic pressure-volume relation at end-diastole. EDP indicates end-diastolic pressure; EDV, end-diastolic volume; ESV, end-systolic volume; Piso, max pressure of an isovolumic beat; RVESP, right ventricular end-systolic pressure; RV-PA, right ventricular-pulmonary artery; and SV, stroke volume. Figure created with BioRender.com.

[dP/dtmax]) and the isovolumic relaxation period (from minimal dP/dt to start diastole) by a semiautomatic MATLAB R2008a program (The MathWorks, Natick, MA). Right ventricular end-systolic pressure was estimated by 1.65×mPAP—7.79.[28] Stroke volume was derived from CMR. Pressure data were averaged over several beats to reduce respiratory variations.

Arterial elastance (Ea), a measure of RV afterload, was calculated as:

$$Ea = \frac{\text{RVESP}}{SV}$$

RV-PA coupling was then calculated as Ees over Ea. Diastolic stiffness (Figure 1) was assessed by end-diastolic elastance (Eed). The diastolic pressure-volume relationship was determined at end-diastole as described previously.[22,29] Reference values (n=38) for pressure-volume derived Eed were derived from a historical group of healthy control subjects who were referred for unexplained dyspnea/evaluation of PH (Table S1; n=32 RVEF >50% and mPAP<20 mm Hg, PVR <240 dynes/s/cm^5) or subjects with positive BMPRII (bone morphogenetic protein receptor type II) mutation carrier status (n=6 RVEF >55% and mPAP <20 mm Hg, PVR <240 dynes/s/cm^5), but normal pulmonary artery pressures.

Cardiac MRI

Cardiac MRI was performed on a 1.5 T Avanto or Sola scanner (Siemens Healthcare, Erlangen, Germany). T1 mapping was performed on basal and mid-ventricular short-axis images for evaluation of RV diffuse interstitial fibrosis using a 5-5-3 modified look-locker inversion recovery.[30] Typical steady-state free

precession parameters were repetition time/time to echo 3.6/1.12 ms, flip angle 35°, voxel size 1.4×1.4×8 mm, and images were acquired with a slice thickness of 8.0 mm. The T1 values delivered by our MRI scanner were verified by using the QalibreMD phantom model 130,[31] which provides ground-truth T1 values in the range between 30 and 2000 ms. On this phantom, we applied the same MRI pulse sequence that we used in the patients.

To measure T1 relaxation time in the relatively thin-walled RV, the image acquisition used for T1 mapping was performed at the end of systole, when the RV free wall (RVFW) reaches its highest thickness.

After measurement of the native T1 map, a dose of 0.3 mmol/kg gadoterate meglumine (Dotarem) was administered intravenously, with injection rate of 3 mL/s, flushed with 20-mL saline. Ten minutes after the contrast injection, the T1 measurements were repeated at the same slice locations using the same parameters. Acquisition and analyses of ventricular volumes were performed as previously reported using commercially available software (Circle CVI42).[25] Relative wall thickness was calculated by dividing RV mass by RV end-diastolic volume. Volumes and mass were indexed to body surface area. Reference values for CMR-derived ventricular mass was derived from the same historical cohort as described for the pressure-volume loop analysis (Table S1).

CMR Image Analysis

T1 mapping and ECV analysis was performed by using commercially available software (Medis Suite 3.2). Image analyses was performed in a random order by an experienced pulmonologist in training with 8 years of experience in respiratory and cardiovascular imaging and subsequently was double checked by a clinical researcher with 4 years of experience in cardiac MRI. Beforehand, both researchers received extensive training by an EBCR cardiothoracic radiologist with more than 20 years of experience. In the myocardial modified look-locker inversion recovery images, the same myocardial regions were delineated before and after contrast application (Figure 2; Figure S2). Thus the subsequent ECV calculation is based on the relaxivity difference post- versus precontrast, within the same region. Regions of interest consisted of (1) RVFW, (2) anterior RV interventricular insertion point (RVIP), (3) posterior RVIP, (4) interventricular septum, and (5) LV free wall.[32] Regions of interest, used for the T1 quantification, were drawn to be as large as possible, while avoiding any inclusion of subendocardial blood, papillary muscles, trabeculae, and subepicardial tissue (Figure 2; Figure S2). The regions of interest of the RV were drawn in the lateral or inferior RV free wall (12–24 voxels, corresponding to an in-plane size in the range of 16.8–33.6 mm^2). T1-maps were assessed for quality by examination of the original images used for T1 calculation, and R^2 maps as indicators for the quality of the T1 fitting. Blood T1 time was derived from the mean of regions of interest drawn in the blood pool of the LV cavity in basal and mid-ventricular short-axis slices. Hematocrit was obtained the same day of the right heart catheterization. The extracellular volume fraction, a measure of diffuse interstitial fibrosis, was quantified from the pre- and postcontrast T1 relaxation times and was calculated as described previously:[33,34]

$$ECV = (1 - \text{hematocrit}) \frac{\left(\frac{1}{T1_{myo,post}}\right) - \left(\frac{1}{T1_{myo,pre}}\right)}{\left(\frac{1}{T1_{blood,post}}\right) - \left(\frac{1}{T1_{blood,pre}}\right)}$$

Total RV matrix and cell volumes were calculated from the product of RV myocardial volume (RV mass divided by the specific mass of myocardium=1.05 g/mL) and ECV or (1—ECV), respectively.[10]

Biomarkers

Blood was transferred immediately after collection into a glass tube and allowed to clot. Serum was separated from the blood cells by centrifugation at 3000 rpm for 10 minutes; supernatant was collected and immediately stored at −80 °C until simultaneous analysis. Total protein concentrations of MMP-1 (matrix metalloproteinase 1; DY901B) and TIMP-1 (tissue inhibitor of metalloproteinase-1; DTM100) were measured using Solid Phase Sandwich ELISAs (R & D Systems, Inc, Minneapolis, MN) per manufacturer's protocol. In addition, we determined active TGF-β1 (transforming growth factor-β1) protein concentrations using the human TGF- β Duo set ELISA kit (DY240) and Sample activation Kit 1 (DY010; R & D Systems Inc., Minneapolis, MN) per manufacturer's protocol. Reference values were derived from mean values of control subjects as described previously.[35–37]

Statistical Analysis

Data are presented as mean±SD, median (25th–75th percentiles), or number of patients (%). All variables were tested for normal distribution by carefully assessing the mean, median, and SD. Data that failed the normal distribution were log- (Eed, TIMP-1, MMP-1/TIMP-1 ratio) or square root (Ea, Ees, Ees/Ea, TGF-β) transformed for analysis. Comparisons of characteristics before, and 6 and 18 months after PEA were performed using paired *t* test with Bonferroni correction, where 0.05 was divided by the number of comparisons being made to determine statistical significance. Comparisons of characteristics between patients and healthy controls were performed using unpaired *t* test with Bonferroni correction. If the data were not distributed normally the Wilcoxon signed-rank test (Eed/relative wall thickness, MMP-1) was used. The interaction between time (baseline versus 6-month follow-up) and RVFW components (cell or matrix volume) was assessed with a repeated-measures ANOVA. Missing data were not imputed. Statistical analyses were performed using R version 3.6.3.

RESULTS

Baseline Characteristics

As indicated in the flowchart (Figure S3), 33 patients with CTEPH fulfilled the in- and exclusion criteria. Follow-up measurements were incomplete in 4 patients, and 4 patients who were assessed for eligibility were finally not enrolled, resulting in 25 patients with measurements at baseline, 6 months and 18 months after PEA. Baseline characteristics are presented in Table 1. Mean age at CTEPH diagnosis was 62±12 years, and there was a predominance of males (60%). Most frequently observed comorbidities were hypertension (32%) and ischemic heart disease (12%). A history of acute pulmonary embolism or both venous thromboembolism and acute pulmonary embolism was present in 60% and 32% of patients, respectively. Pulmonary hemodynamics improved 6

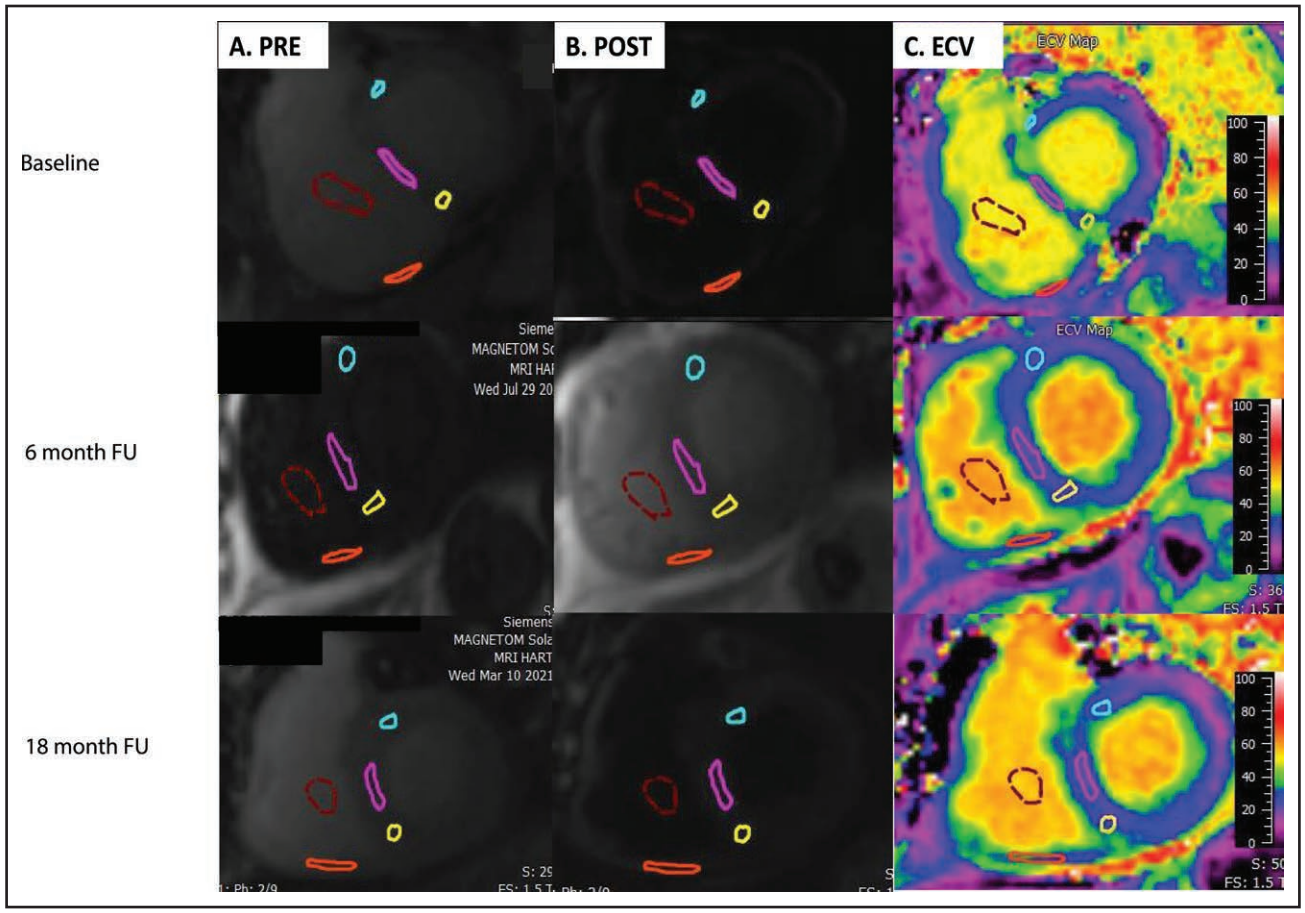

Figure 2. An example of basal ventricular short-axis pre- and postcontrast modified look-locker inversion recovery (MOLLI) images and extracellular volume fraction (ECV) map of a patient at baseline and during long-term follow-up after pulmonary endareterectomy (PEA).

T1 measurements were made within regions of interest (ROIs) of the right ventricular (RV) free wall (orange), septum (purple), anterior (blue), and posterior (yellow) insertion points in the native and postcontrast MOLLI images and ECV was calculated. Although the RV free wall thickness reduces after PEA, it was possible to determine ROIs of the RV free wall.

months after PEA, as indicated by a decrease in mPAP from 45±11 to 24±9 mm Hg (−21.1 mm Hg [95% CI, −26.0 to −16.2]; $P<0.0001$), PVR from 561 (427–711) to 132 (112–194) dynes/s/cm^5 ($P<0.0001$), mean right atrial pressure from 8 (6–10) to 5 (3–6) mm Hg ($P<0.01$) and an increase in cardiac index from 2.6±0.6 to 3.0±0.6 L/min per m^2 (0.4 L/min per m^2 [95% CI, 0.1–0.6]; $P<0.05$; Table S2). Residual PH after PEA was present in 4 (16%) patients. None of these patients received interventional treatment after surgery. RVEF increased from 41±14 to 52±9% (10.2% [95% CI, 5.7–14.7]; $P<0.01$) 6 months after PEA and indexed RVEDV decreased from 91±28 to 71±13 mL/m^2 (−20.1 mL/m^2 [95% CI, −29.5 to −10.7]; $P<0.0001$).

RV Mass and Diastolic Stiffness

Indexed RV mass decreased from 43±15 to 27±11g/m^2 (−15.9 g/m^2 [95% CI, −21.4 to −10.5]; $P<0.0001$) 6 months after PEA and stabilized to a somewhat elevated level at 18 months after PEA 28±9 versus 22±6 g/m^2 in healthy controls (95% CI, 2.1–9.8; $P<0.01$; Figure 3A). RV diastolic stiffness (Eed) had normalized 6 months after PEA ($P=0.07$; Figure 3B). To assess whether the improvement of Eed was mainly driven by a reduction in RV hypertrophy, Eed values were corrected for relative wall thickness (Figure 3C).[22] Indeed, Eed corrected for relative wall thickness did not significantly reduce after PEA ($P=0.09$), indicating that the improvements in diastolic stiffness are a reflection of reduced RV hypertrophy. No further changes were observed between 6 and 18 months after PEA. Compared with the values of healthy controls, Eed corrected for relative wall thickness was increased before PEA (1.02 [0.68–2.44] versus 0.63 [0.45–0.78]; $P<0.01$ in healthy controls), but normalized 6 months after PEA (0.66 [0.33–0.97]; $P=0.6$).

Systolic Right Ventricular Adaptation

Before surgery RV afterload (Ea) was elevated (Figure 3D) and decreased 6 months after PEA (decreased from 0.88 [0.72–1.22] to 0.29 [0.25–0.41] mm Hg/mL;

Table. Baseline Characteristics

General	N=25
Age, y	62±12
Male sex (n, %)	15 (60)
BMI, kg/m^2	28±5
Comorbidities (n, %)	
DM	1 (4)
Hypertension	8 (32)
Ischemic heart disease	3 (12)
Renal disease	1 (4)
Other	8 (32)
History of VTE (n, %)	
DVT	2 (8)
PE	15 (60)
DVT and PE	8 (32)
Functional	
NYHA Fc, (n)	
I/II/III/IV	0/12/10/3
NT-proBNP, ng/mL	286 (132–1455)
6MWD, m	414 (376–484)
Hemodynamics	
mPAP, mm Hg	45±11
PVR, dynes/s/cm^5	561 (427–711)
Ea, mm Hg/mL	0.88 (0.72–1.22)
Ees, mm Hg/mL	0.40 (0.27–0.68)
Ees/Ea	0.49 (0.37–0.64)
Eed, mm Hg/mL	0.57 (0.29–0.85)
Eed/RWT, mm Hg/mL per g	0.71 (0.68–2.45)
Cardiac MRI	
Indexed RVEDV, mL/m^2	91±28
Indexed RVESV, mL/m^2	57±28
RVEF, %	41±14
Indexed RV mass, g/m^2	43±15
RV RWT, g/mL	0.48±0.17

Data are presented as mean±SD, median (IQR), or n (%). 6MWD indicates 6-minute walking distance; BMI, body mass index; DM, diabetes mellitus; DVT, deep venous thrombosis; Eed, end-diastolic stiffness; Ees, end-systolic elastance; IQR, interquartile range; mPAP, mean pulmonary arterial pressure; MRI, magnetic resonance imaging; NT-proBNP, N-terminal pro-B-type natriuretic peptide; NYHA Fc, New York Heart Association Functional Classification; PE, pulmonary embolism; PVR, pulmonary vascular resistance; RV RWT, right ventricular relative wall thickness; RVEDV, right ventricular end-diastolic volume; RVEF, right ventricular ejection fraction; RVESV, right ventricular end-systolic volume; and VTE, venous thromboembolism.

P<0.0001). Compared with healthy controls, RV contractility (Ees) was increased at baseline (Figure 3E; 0.40 [0.27–0.68] versus 0.30 [0.19–0.38]; P<0.01 in healthy controls) and normalized 6 months after PEA (0.22 [0.15–0.31] mm Hg/mL; P=0.4). Taken together, this resulted in no changes in RV-arterial coupling before and after PEA (P=0.2; Figure 3F). No further changes were observed between 6 and 18 months after PEA.

ECV Measures of RVFW Remain Increased After PEA

RVFW ECV mapping was successfully performed in 22 of 25 patients (88%) at baseline, 20 of 25 (80%) at 6 months, and 24 of 25 (96%) at 18 months. At baseline, ECV values of the RVFW and anterior and posterior RVIP were elevated compared with the ECV values of the LV free wall and septum (Tables S3 and S4). ECV in RVFW increased significantly 6 months after PEA (3.6% [95% CI, 1.2–6.1]; P=0.013) and remained elevated until 18 months of follow-up (Table S3; Figure 4A). ECV mapping separates the myocardium into cell and matrix compartments, therefore, making it possible to make a distinction between cellular and extracellular matrix volume.[10] As demonstrated in Figure 4B and 4C, the increased ECV in RVFW at 6 and 18 months was explained by a differential response of matrix and cell volume. Although both matrix and cell volume were reduced after PEA and contributed to the reduction in RV mass, the reduction in cell volume (cardiomyocyte size/hypertrophy) was larger than the reduction in matrix volume ($P_{interaction}$=0.0013). As a result, the relative proportion of extracellular volume in the RV increased after PEA. In contrast to ECV in RVFW, native T1 in RVFW was elevated at baseline but decreased significantly (Table S4).

ECV of the anterior and posterior RVIP remained stable or decreased after PEA (Table S3). As shown in Figure 5, ECV of basal short axis in both anterior and posterior RVIP remained elevated 6 months after PEA. However, after 18 months of follow-up, both anterior (−2.7 [95% CI, −4.5 to −0.8]; P<0.01) and posterior RVIP decreased significantly (−4.1 to −0.4; P<0.01). As with ECV mapping, T1 relaxation time of the anterior and posterior RVIP remained stable or decreased after PEA (Table S4).

Collagen Synthesis Dominates Over Collagen Breakdown

To determine the contribution of collagen metabolism, we subsequently analyzed biomarkers of collagen synthesis and breakdown at baseline, and 6 and 18 months after PEA. Levels of MMP-1 and its inhibitor TIMP-1 were elevated at baseline and remained elevated after PEA relative to reference values.[20,36,38] In addition, TIMP-1 levels were relatively higher and remained higher at follow-up compared with MMP-1 levels, as indicated by the MMP-1/TIMP-1 ratio in Figure 6. Active TGF-β levels were elevated at baseline and did not change significantly 6 and 18 months after PEA.

DISCUSSION

In this prospective study in patients with CTEPH undergoing PEA, we show that (Figure 7):

1. Although RV mass decreases after PEA, it does not completely normalize.

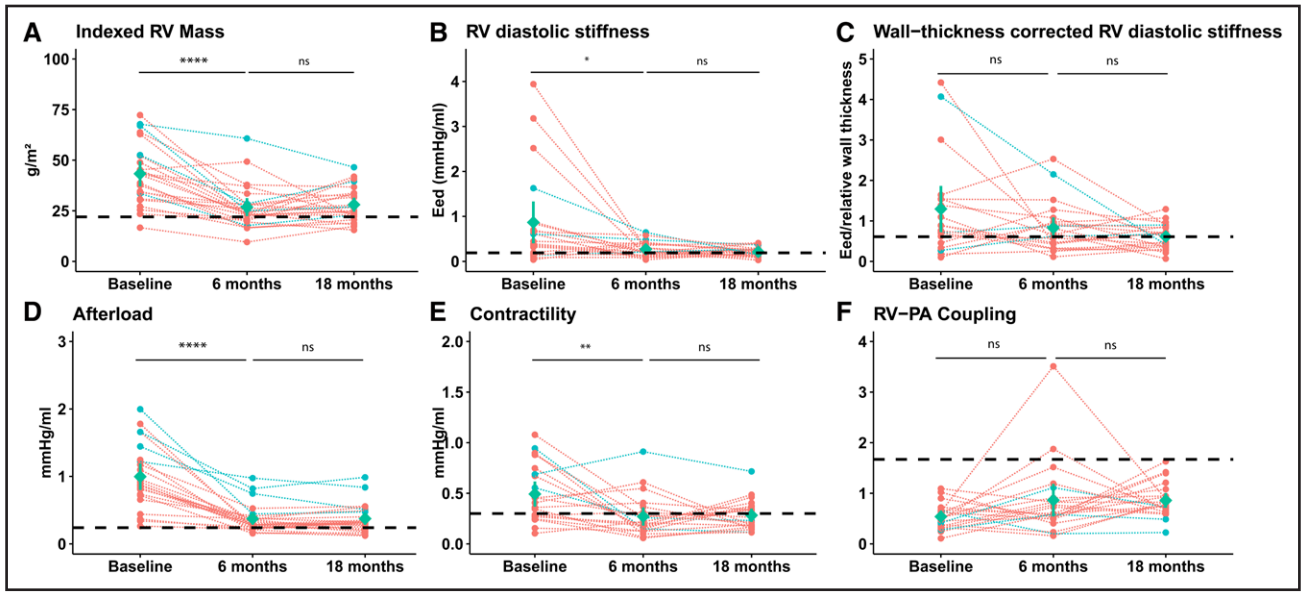

Figure 3. Long-term changes in right ventricular (RV) mass, diastolic stiffness, and systolic adaptation.
A, RV mass reduces but does not completely normalize over time compared with healthy controls. **B**, RV diastolic stiffness reduces and is comparable with healthy controls at 6 and 18 months. **C**, RV diastolic stiffness corrected for wall thickness did not significantly reduce over time indicating that the improvements in diastolic stiffness are a reflection of reduced RV hypertrophy. **D**, RV afterload was elevated and decreased at 6 and 18 months. **E**, RV contractility was increased compared with healthy controls and normalizes at 6 and 18 months. **F**, No change in right ventricular-pulmonary arterial (RV-PA) coupling before and after pulmonary endarterectomy (PEA). Data are presented as individual data points. No PH: patients without residual pulmonary hypertension 6 months after PEA; residual PH: patients with residual pulmonary hypertension 6 months after PEA; statistical tests: paired *t* test with Bonferonni correction (indexed RV mass, end-diastolic stiffness [Eed], arterial elastance [Ea], end-systolic elastance [Ees], Ees/Ea) and Wilcoxon signed-rank test (wall thickness corrected Eed). Data are presented as individual data points. Statistical tests: paired *t* test with Bonferonni correction (Eed, indexed RV mass) and Wilcoxon signed-rank test (wall thickness corrected Eed). The dashed line represents the mean value of healthy controls. Blue lines represents residual PH patients. The green triangles represent the mean values over time. PH indicates pulmonary hypertension.

2. Due to a relatively smaller decrease in matrix volume compared with the decrease in cellular volume, ECV in RVFW increases after PEA indicating persistent RV diffuse interstitial fibrosis after PEA.
3. Circulating levels of TIMP-1 and active TGF-β are increased, and MMP-1/TIMP-1 ratio is decreased both before and after surgery, indicating that collagen synthesis dominates over collagen breakdown.
4. Although RV mass, ECV in RVFW, and collagen synthesis biomarkers remain increased after PEA, they do not affect RV systolic function and diastolic stiffness after PEA.

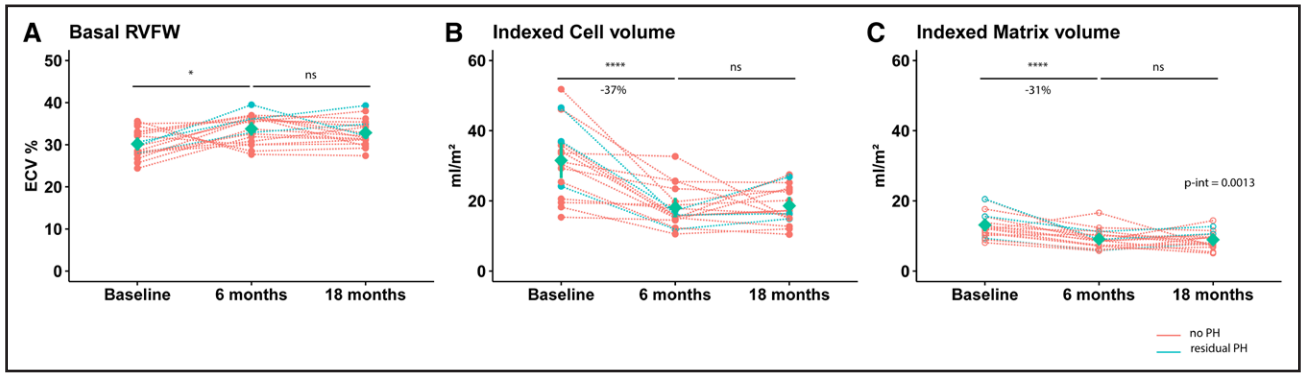

Figure 4. Long-term changes in cellular and extracellular matrix by cardiac magnetic resonance (CMR) of the basal right ventricle.
A, Basal extracellular volume fraction (ECV) right ventricular free wall (RVFW) is elevated at baseline and increases at 6 months. ECV mapping separates the myocardium into cell (**B**) and matrix components (**C**). The increased ECV was explained by a larger reduction in indexed cell volume (**B**) compared with indexed matrix volume (**C**). Data are presented as individual data points. No PH: patients without residual pulmonary hypertension 6 months after pulmonary endarterectomy (PEA); residual PH: patients with residual pulmonary hypertension 6 months after PEA. Statistical tests: paired *t* test with Bonferonni correction. The interaction between time (baseline vs 6 mo follow-up) and RV free wall components (cell or matrix volume) was assessed with a repeated-measures ANOVA. Blue lines represents residual PH patients. The green triangles represent the mean values over time. PH indicates pulmonary hypertension.

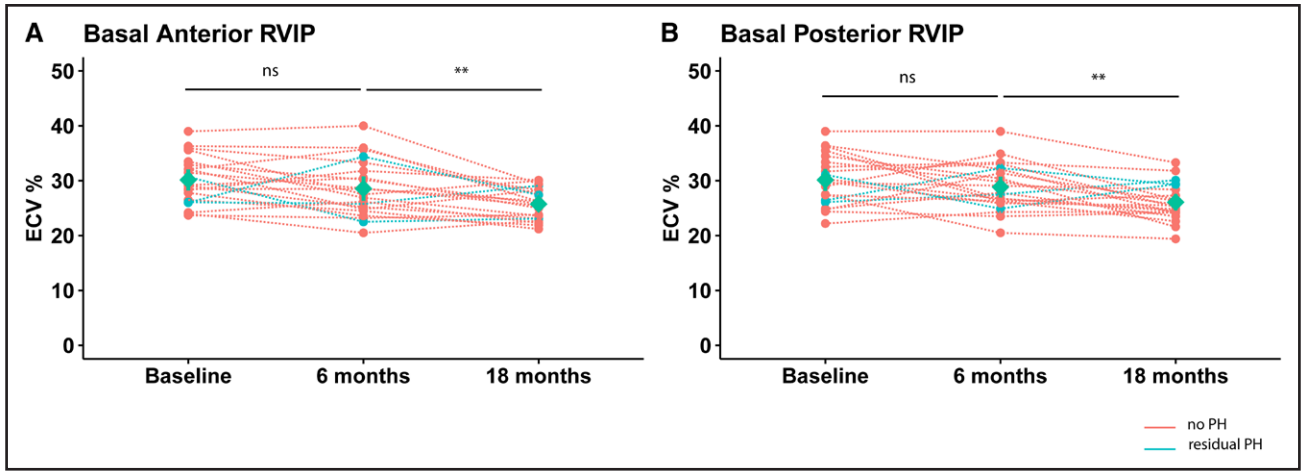

Figure 5. Long-term changes in extracellular volume fraction of the septum.
Extracellular volume fraction (ECV) of basal short axis in both anterior (**A**) and posterior (**B**) right ventricular interventricular insertion point (RVIP) remained elevated 6 months after pulmonary endarterectomy (PEA). At 18 months of follow-up, both anterior and posterior RVIP decreased significantly. Data are presented as individual data points. No PH: patients without residual pulmonary hypertension 6 months after PEA; residual PH: patients with residual pulmonary hypertension 6 months after PEA; statistical tests: paired *t* test with Bonferonni correction. Blue lines represents residual PH patients. The green triangles represent the mean values over time. PH indicates pulmonary hypertension.

Reverse Remodeling of RV After Pressure Unloading by PEA

RV hypertrophy, increased stiffening of RV sarcomeres, and collagen deposition are known to increase ventricular stiffness in PAH.[22,29,39] Whether these alterations can recover after pressure unloading was not previously studied. PEA in patients with CTEPH provides the unique opportunity to study potential reverse remodeling after pressure unloading. In this study, we therefore investigated RV morphology, function, and collagen metabolism at baseline before PEA, and 6 and 18 months after PEA.

Although RV mass and RV systolic function and diastolic stiffness both significantly decreased after PEA, we showed that RV mass remained increased 6 and 18 months after PEA compared with healthy controls. In addition, RV fibrosis determined by ECV measurements did not regress in the RV free wall, whereas regression of RV fibrosis was observed in the insertion points. It could be hypothesized that hypertrophic and fibrotic regression requires a longer period of time beyond 18 months.[7,10] Other possible explanations for residual RV fibrosis despite pressure unloading are irreversible damage or residual pressure overload at rest or during exercise. However, the decrease in MMP-1 to TIMP-1 ratio and the increase in active TGF-β levels at baseline but also after PEA, suggest an ongoing collagen turnover, which is not affected by reducing RV pressure. Residual PH was diagnosed in only 4 patients. Although RV mass, ECV in RVFW and collagen synthesis biomarkers remained increased after PEA, they were not associated with disturbed RV systolic function and diastolic stiffness. As such, the clinical implications of residual RV remodeling after PEA for CTEPH are unclear.

ECV Measure of the RVFW as an Imaging Biomarker for RV Fibrosis

Expansion of the extracellular matrix volume is initiated by pathological modifications of the extracellular matrix and reflects diffuse interstitial fibrosis or edema in PH. Previously, T1-mapping was used to detect diffuse interstitial fibrosis, which has been shown to have prognostic value in PH.[32] However, native T1-mapping is limited by wide variation, which can affect reproducibility.[14] ECV provides more robust measurements for diffuse interstitial fibrosis compared with T1 mapping.[14] However, it has been challenging to assess the thin-walled RVFW for diffuse interstitial fibrosis by cardiac MRI and, therefore, only data regarding ECV of the septum and RVIPs have been reported in patients with CTEPH.[2] The present study is the first study assessing ECV in the relatively thin-walled RV after PEA. By measuring ECV at end systole, we were able to demonstrate elevated ECV in RVFW as well as in the anterior and posterior RVIPs after PEA.

We observed increased ECV values in the RVFW 6 and 18 months after PEA, whereas ECV values of RVIPs normalized. This increase in ECV in the free wall after PEA may be explained by a larger reduction in cell volume relative to matrix volume, similar to previous data in left heart disease.[10] The normalization in the RVIPs is consistent with prior findings of elevated T1- and ECV values of the RVIPs in PH, due to the high amount of force and traction especially the septum and RVIPs undergo myocardial remodelling.[40–43] It is therefore likely that normalization of the RVIPs occurred with improvement of afterload and hemodynamic parameters.

In contrast to ECV in RVFW, we showed that native T1 in RVFW decreased after PEA. This might be

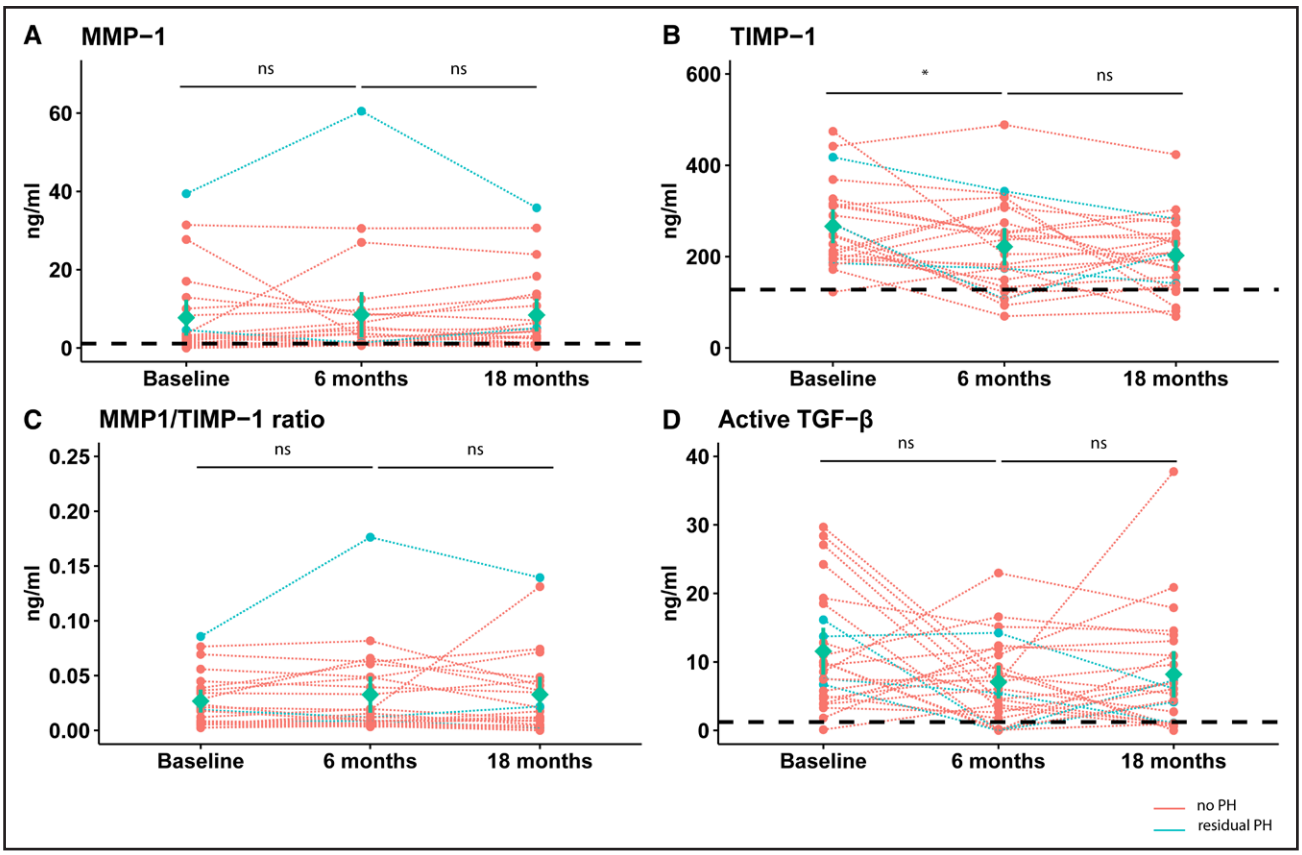

Figure 6. Circulating collagen biomarkers.
Levels of MMP-1 (matrix metalloproteinase 1; **A**) and its inhibitor TIMP-1 (tissue inhibitor of metalloproteinase-1; **B**) were elevated at baseline and remained elevated after pulmonary endareterectomy (PEA) relative to reference values. TIMP-1 levels were relatively higher and remained higher at follow-up compared with MMP-1 levels, as indicated by the MMP-1/TIMP-1 ratio (**C**). Active TGF-β (transforming growth factor-β; **D**) levels were elevated at baseline and did not change significantly 6 and 18 months after PEA. Data are presented as individual data points. No PH: patients without residual pulmonary hypertension 6 months after PEA; residual PH: patients with residual pulmonary hypertension 6 months after PEA. Statistical tests: paired *t* test with Bonferonni correction. The dashed line represents the mean value of healthy controls adapted from Safdar,[35] Dziadzio et al,[37] and Karapanagiotidis et al.[38] Blue lines represents residual PH patients. The green triangles represent the mean values over time. PH indicates pulmonary hypertension.

explained by the different compartments that T1 and ECV measure. Native T1 is composed of both the cellular and ECM compartment, whereas ECV measures only the ECM compartment. Taken together, our study is among the first to demonstrate that ECV measured in the RVFW remains increased after PEA and may indicate that diffuse interstitial fibrosis regression is not complete in the RV.

Limitations

Our study is limited by the relatively small sample size of patients with CTEPH. Nevertheless, patients were prospectively included and followed over a time of 18 months after PEA, generating an unique data set that allowed us to study long-term RV reverse remodeling. In addition, we studied systemic biomarkers for RV fibrosis. We measured collagen synthesis and degradation biomarkers in serum samples of CTEPH patients at baseline, and 6 and 18 months after PEA. Although these biomarkers reflect collagen turn over, it is difficult to determine the origin of the secreted biomarkers. It is impossible to know whether systemic alterations in the collagen metabolism reflect local changes within the RV or pulmonary vasculature. In addition, active collagen turnover has been described in various fibrotic conditions as well. Although we did not provide direct evidence, none of our patients had a chronic fibrotic condition or concomitant left heart disease. Ideally pressures and volumes are measured simultaneously (eg, with a conductance catheter). However, in our study, pressures and volumes were derived from a fluid-filled catheter and CMR, respectively. Finally, one explanation for the remaining RV fibrosis could be that a portion of patients have residual PH after PEA. However, as depicted in the figures (blue lines represents residual PH patients), no differences in RV mass, RV diastolic stiffness, or RV fibrosis were observed at 6 and 18 months between patients with and without residual PH.

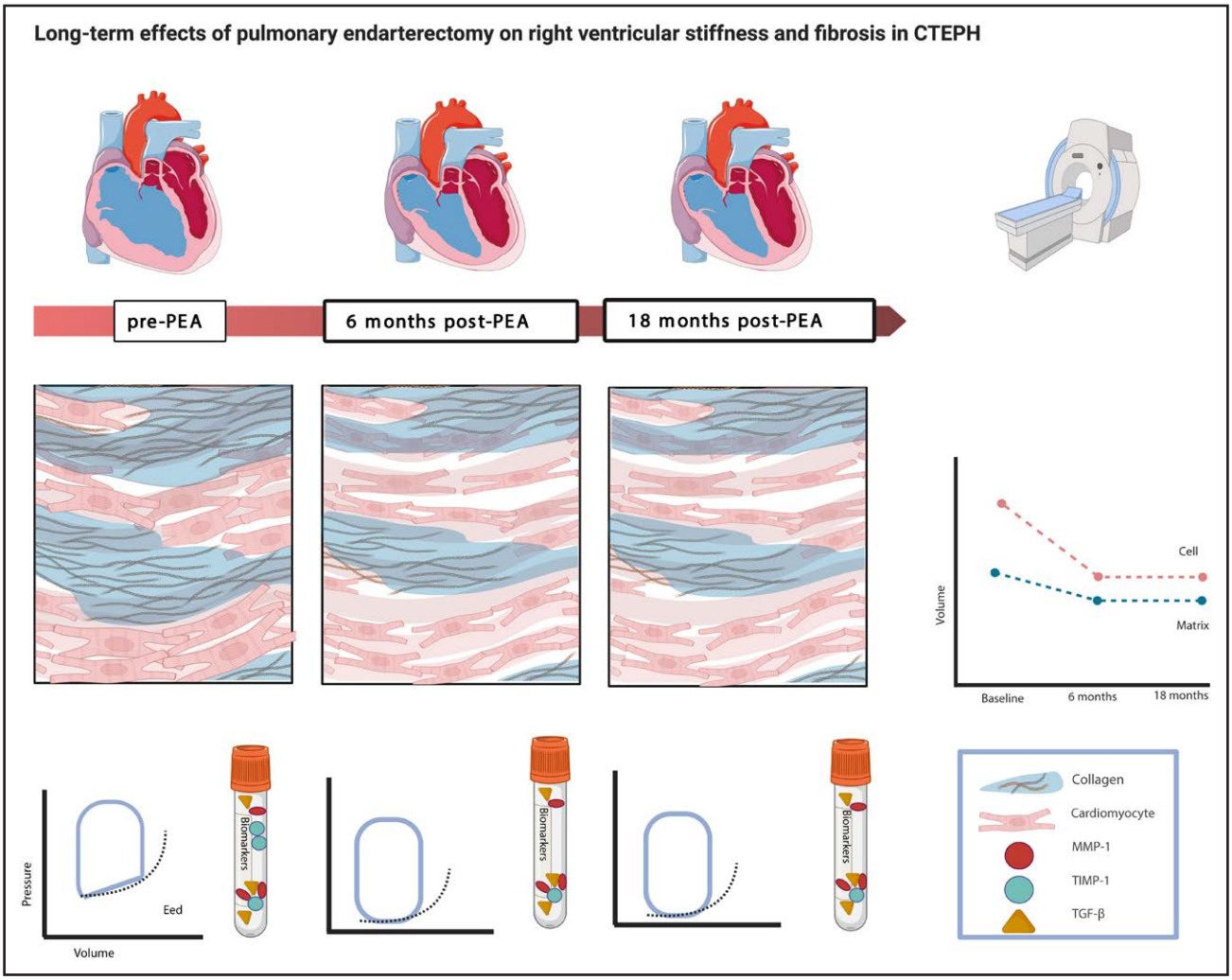

Figure 7. Schematic presentation of the main results.
Right ventricular (RV) mass reduces but does not completely normalize over time compared with healthy controls. After pulmonary endareterectomy (PEA), extracellular matrix regression is not complete in the RV as indicated by a relative smaller decrease in matrix volume compared with cellular volume. This was accompanied by elevated levels of collagen biomarkers suggestive of an active collagen turnover. Nevertheless, this did not affect the diastolic stiffness. MMP-1 indicates matrix metalloproteinase 1; TGF-β, transforming growth factor-β; and TIMP-1, tissue inhibitor of metalloproteinase-1. Figure created with BioRender.com.

Conclusions

Although cellular hypertrophy regresses and systolic and diastolic stiffness normalizes after PEA, ECV in RVFW remains elevated and is the result of a relatively smaller decrease in extracellular matrix compared with cellular volume. In addition, circulating levels of collagen biomarkers were increased both pre- and post-surgery in patients with CTEPH. Taken together, these findings suggest that even after successful PEA, diffuse interstitial fibrosis regression is not complete in the RV and signs of active collagen turnover are observed at 6 and 18 months after PEA.

ARTICLE INFORMATION

Received November 12, 2022; accepted July 17, 2023.

Affiliations

Amsterdam UMC location Vrije Universiteit Amsterdam, PHEniX Laboratory, Department of Pulmonary Medicine, the Netherlands (N.J.B., A.K., J.v.W., J.N.W., S.M.A.J., A.B., E.J.N., A.V.N., F.S.d.M., H.J.B.). Amsterdam Cardiovascular Sciences, Pulmonary Hypertension and Thrombosis, the Netherlands (N.J.B., A.K., J.v.W., J.N.W., S.M.A.J., E.J.N., J.T.M., A.V.N., F.S.d.M., H.J.B., L.J.M.). Department of Cardiology, Aarhus University Hospital, Denmark (S.A., A.A.). Amsterdam UMC location Vrije Universiteit Amsterdam, Department of Radiology and Nuclear Medicine, the Netherlands (J.T.M., L.J.M.). Department of Internal Medicine, Chest Unit, Suez Canal University, School of Medicine, Ismailia, Egypt (A.A.B.). Department of Molecular Cell Biology, Leiden University Medical Centre, the Netherlands (C.B., M.-J.G.).

Acknowledgments

Drs Meijboom, Bogaard, de Man, Vonk Noordegraaf, Andersen, Andersen, and Braams designed the study. Drs Meijboom, Bogaard, de Man, Wessels, Goumans, Vonk Noordegraaf, Marcus, Kianzad, and Braams wrote the article. Drs Braams, Kianzad, Wessels, Jansen, Andersen, Andersen, Boonstra, Nossent, and Bayoumy and J. van Wezenbeek and C. Becher collected the data. Drs Braams, Kianzad, Wessels, Jansen, Andersen, Andersen, Bayoumy, Nossent, Bayoumy, Meijboom, Bogaard, de Man, Goumans, Marcus, and Vonk Noordegraaf and

J. van Wezenbeek and C. Becher performed data analyses and interpretation. All authors provided critical comments on the article.

Sources of Funding

This investigator-sponsored trial was financially supported by the Netherlands CardioVascular Research Initiative: CVON-2017-10 DOLPHIN-GENESIS (Drs Vonk Noordegraaf, de Man, and Bogaard) and Janssen-Cilag B.V.

Disclosures

All authors certify that they have no affiliations with or involvement in any organization or entity with any financial interest (such as honoraria; educational grants; participation in speakers' bureaus; membership, employment, consultancies, stock ownership, or other equity interest; and expert testimony or patent-licensing arrangements) or nonfinancial interest (such as personal or professional relationships, affiliations, knowledge, or beliefs) in the subject matter or materials discussed in this article.

Supplemental Material

Tables S1–S4
Figures S1–S3

REFERENCES

1. Galiè N, Humbert M, Vachiery JL, Gibbs S, Lang I, Torbicki A, Simonneau G, Peacock A, Vonk Noordegraaf A, Beghetti M, et al; ESC Scientific Document Group. 2015 ESC/ERS Guidelines for the diagnosis and treatment of pulmonary hypertension: The Joint Task Force for the Diagnosis and Treatment of Pulmonary Hypertension of the European Society of Cardiology (ESC) and the European Respiratory Society (ERS): Endorsed by: Association for European Paediatric and Congenital Cardiology (AEPC), International Society for Heart and Lung Transplantation (ISHLT). *Eur Heart J*. 2016;37:67–119. doi: 10.1093/eurheartj/ehv317
2. Roller FC, Wiedenroth C, Breithecker A, Liebetrau C, Mayer E, Schneider C, Rolf A, Hamm C, Krombach GA. Native T1 mapping and extracellular volume fraction measurement for assessment of right ventricular insertion point and septal fibrosis in chronic thromboembolic pulmonary hypertension. *Eur Radiol*. 2017;27:1980–1991. doi: 10.1007/s00330-016-4585-y
3. Vonk-Noordegraaf A, Haddad F, Chin KM, Forfia PR, Kawut SM, Lumens J, Naeije R, Newman J, Oudiz RJ, Provencher S, et al. Right heart adaptation to pulmonary arterial hypertension: physiology and pathobiology. *J Am Coll Cardiol*. 2013;62:D22–D33. doi: 10.1016/j.jacc.2013.10.027
4. Vonk Noordegraaf A, Westerhof BE, Westerhof N. The relationship between the right ventricle and its load in pulmonary hypertension. *J Am Coll Cardiol*. 2017;69:236–243. doi: 10.1016/j.jacc.2016.10.047
5. Bogaard HJ, Abe K, Vonk Noordegraaf A, Voelkel NF. The right ventricle under pressure: cellular and molecular mechanisms of right-heart failure in pulmonary hypertension. *Chest*. 2009;135:794–804. doi: 10.1378/chest.08-0492
6. Reesink HJ, Marcus JT, Tulevski II, Jamieson S, Kloek JJ, Vonk Noordegraaf A, Bresser P. Reverse right ventricular remodeling after pulmonary endarterectomy in patients with chronic thromboembolic pulmonary hypertension: utility of magnetic resonance imaging to demonstrate restoration of the right ventricle. *J Thorac Cardiovasc Surg*. 2007;133:58–64. doi: 10.1016/j.jtcvs.2006.09.032
7. D'Armini AM, Zanotti G, Ghio S, Magrini G, Pozzi M, Scelsi L, Meloni G, Klersy C, Viganò M. Reverse right ventricular remodeling after pulmonary endarterectomy. *J Thorac Cardiovasc Surg*. 2007;133:162–168. doi: 10.1016/j.jtcvs.2006.08.059
8. Berman M, Gopalan D, Sharples L, Screaton N, Maccan C, Sheares K, Pepke-Zaba J, Dunning J, Tsui S, Jenkins DP. Right ventricular reverse remodeling after pulmonary endarterectomy: magnetic resonance imaging and clinical and right heart catheterization assessment. *Pulm Circ*. 2014;4:36–44. doi: 10.1086/674884
9. Lamb HJ, Beyerbacht HP, de Roos A, van der Laarse A, Vliegen HW, Leujes F, Bax JJ, van der Wall EE. Left ventricular remodeling early after aortic valve replacement: differential effects on diastolic function in aortic valve stenosis and aortic regurgitation. *J Am Coll Cardiol*. 2002;40:2182–2188. doi: 10.1016/s0735-1097(02)02604-9
10. Treibel TA, Kozor R, Schofield R, Benedetti G, Fontana M, Bhuva AN, Sheikh A, López B, González A, Manisty C, et al. Reverse myocardial remodeling following valve replacement in patients with aortic stenosis. *J Am Coll Cardiol*. 2018;71:860–871. doi: 10.1016/j.jacc.2017.12.035
11. Maestrini V, Treibel TA, White SK, Fontana M, Moon JC. T1 mapping for characterization of intracellular and extracellular myocardial diseases in heart failure. *Curr Cardiovasc Imaging Rep*. 2014;7:9287–9294. doi: 10.1007/s12410-014-9287-8
12. Flett AS, Hayward MP, Ashworth MT, Hansen MS, Taylor AM, Elliott PM, McGregor C, Moon JC. Equilibrium contrast cardiovascular magnetic resonance for the measurement of diffuse myocardial fibrosis: preliminary validation in humans. *Circulation*. 2010;122:138–144. doi: 10.1161/CIRCULATIONAHA.109.930636
13. Kim PK, Hong YJ, Shim HS, Im DJ, Suh YJ, Lee KH, Hur J, Kim YJ, Choi BW, Lee HJ. Serial T1 mapping of right ventricle in pulmonary hypertension: comparison with histology in an animal study. *J Cardiovasc Magn Reson*. 2021;23:64. doi: 10.1186/s12968-021-00755-y
14. Gottbrecht M, Kramer CM, Salerno M. Native T1 and extracellular volume measurements by cardiac MRI in healthy adults: a meta-analysis. *Radiology*. 2019;290:317–326. doi: 10.1148/radiol.2018180226
15. Lee SP, Lee W, Lee JM, Park EA, Kim HK, Kim YJ, Sohn DW. Assessment of diffuse myocardial fibrosis by using MR imaging in asymptomatic patients with aortic stenosis. *Radiology*. 2015;274:359–369. doi: 10.1148/radiol.14141120
16. Nakamori S, Dohi K, Ishida M, Goto Y, Imanaka-Yoshida K, Omori T, Goto I, Kumagai N, Fujimoto N, Ichikawa Y, et al. Native T1 mapping and extracellular volume mapping for the assessment of diffuse myocardial fibrosis in dilated cardiomyopathy. *JACC Cardiovasc Imaging*. 2018;11:48–59. doi: 10.1016/j.jcmg.2017.04.006
17. White SK, Sado DM, Fontana M, Banypersad SM, Maestrini V, Flett AS, Piechnik SK, Robson MD, Hausenloy DJ, Sheikh AM, et al. T1 mapping for myocardial extracellular volume measurement by CMR: bolus only versus primed infusion technique. *JACC Cardiovasc Imaging*. 2013;6:955–962. doi: 10.1016/j.jcmg.2013.01.011
18. Ferreira VM, Wijesurendra RS, Liu A, Greiser A, Casadei B, Robson MD, Neubauer S, Piechnik SK. Systolic ShMOLLI myocardial T1-mapping for improved robustness to partial-volume effects and applications in tachyarrhythmias. *J Cardiovasc Magn Reson*. 2015;17:77–88. doi: 10.1186/s12968-015-0182-5
19. Zhao L, Li S, Ma X, Greiser A, Zhang T, An J, Bai R, Dong J, Fan Z. Systolic MOLLI T1 mapping with heart-rate-dependent pulse sequence sampling scheme is feasible in patients with atrial fibrillation. *J Cardiovasc Magn Reson*. 2016;18:13. doi: 10.1186/s12968-016-0232-7
20. Safdar Z, Tamez E, Chan W, Arya B, Ge Y, Deswal A, Bozkurt B, Frost A, Entman M. Circulating collagen biomarkers as indicators of disease severity in pulmonary arterial hypertension. *JACC Heart Fail*. 2014;2:412–421. doi: 10.1016/j.jchf.2014.03.013
21. Simonneau G, Montani D, Celermajer DS, Denton CP, Gatzoulis MA, Krowka M, Williams PG, Souza R. Haemodynamic definitions and updated clinical classification of pulmonary hypertension. *Eur Respir J*. 2019;53:1801887–1801901. doi: 10.1183/13993003.01913-2018
22. Trip P, Rain S, Handoko ML, van der Bruggen C, Bogaard HJ, Marcus JT, Boonstra A, Westerhof N, Vonk-Noordegraaf A, de Man FS. Clinical relevance of right ventricular diastolic stiffness in pulmonary hypertension. *Eur Respir J*. 2015;45:1603–1612. doi: 10.1183/09031936.00156714
23. Jamieson SW, Kapelanski DP, Sakakibara N, Manecke GR, Thistlethwaite PA, Kerr KM, Channick RN, Fedullo PF, Auger WR. Pulmonary endarterectomy: experience and lessons learned in 1,500 cases. *Ann Thorac Surg*. 2003;76:1457–62; discussion 1462. doi: 10.1016/s0003-4975(03)00828-2.
24. Mayer E, Jenkins D, Lindner J, D'Armini A, Kloek J, Meyns B, Ilkjaer LB, Klepetko W, Delcroix M, Lang I, et al. Surgical management and outcome of patients with chronic thromboembolic pulmonary hypertension: results from an international prospective registry. *J Thorac Cardiovasc Surg*. 2011;141:702–710. doi: 10.1016/j.jtcvs.2010.11.024
25. Trip P, Kind T, van de Veerdonk MC, Marcus JT, de Man FS, Westerhof N, Vonk-Noordegraaf A. Accurate assessment of load-independent right ventricular systolic function in patients with pulmonary hypertension. *J Heart Lung Transplant*. 2013;32:50–55. doi: 10.1016/j.healun.2012.09.022
26. Sunagawa K, Yamada A, Senda Y, Kikuchi Y, Nakamura M, Shibahara T, Nose Y. Estimation of the hydromotive source pressure from ejecting beats of the left ventricle. *IEEE Trans Biomed Eng*. 1980;27:299–305. doi: 10.1109/TBME.1980.326737
27. Spruijt OA, de Man FS, Groepenhoff H, Oosterveer F, Westerhof N, Vonk-Noordegraaf A, Bogaard HJ. The effects of exercise on right ventricular contractility and right ventricular-arterial coupling in pulmonary hypertension. *Am J Respir Crit Care Med*. 2015;191:1050–1057. doi: 10.1164/rccm.201412-2271OC

28. Tello K, Richter MJ, Axmann J, Buhmann M, Seeger W, Naeije R, Ghofrani HA, Gall H. More on single-beat estimation of right ventriculoarterial coupling in pulmonary arterial hypertension. *Am J Respir Crit Care Med*. 2018;198:816–818. doi: 10.1164/rccm.201802-0283LE
29. Rain S, Handoko ML, Trip P, Gan CT, Westerhof N, Stienen GJ, Paulus WJ, Ottenheijm CA, Marcus JT, Dorfmüller P, et al. Right ventricular diastolic impairment in patients with pulmonary arterial hypertension. *Circulation*. 2013;128:2016–25, 1. doi: 10.1161/CIRCULATIONAHA.113.001873
30. Messroghli DR, Moon JC, Ferreira VM, Grosse-Wortmann L, He T, Kellman P, Mascherbauer J, Nezafat R, Salerno M, Schelbert EB, et al. Clinical recommendations for cardiovascular magnetic resonance mapping of T1, T2, T2* and extracellular volume: a consensus statement by the Society for Cardiovascular Magnetic Resonance (SCMR) endorsed by the European Association for Cardiovascular Imaging (EACVI). *J Cardiovasc Magn Reson*. 2017;19:75–99. doi: 10.1186/s12968-017-0389-8
31. CaliberMRI provides robust QA/QC automation software and imaging phantoms, establishing the necessary quantitative MRI (qMRI) calibration framework so qMRI can be implemented in research institutions, clinical sites, hospitals, and imaging centers around the world: https://qmri.com/.
32. Spruijt OA, Vissers L, Bogaard HJ, Hofman MB, Vonk-Noordegraaf A, Marcus JT. Increased native T1-values at the interventricular insertion regions in precapillary pulmonary hypertension. *Int J Cardiovasc Imaging*. 2016;32:451–459. doi: 10.1007/s10554-015-0787-7
33. Moon JC, Messroghli DR, Kellman P, Piechnik SK, Robson MD, Ugander M, Gatehouse PD, Arai AE, Friedrich MG, Neubauer S, et al; Society for Cardiovascular Magnetic Resonance Imaging. Myocardial T1 mapping and extracellular volume quantification: a Society for Cardiovascular Magnetic Resonance (SCMR) and CMR Working Group of the European Society of Cardiology consensus statement. *J Cardiovasc Magn Reson*. 2013;15:92–104. doi: 10.1186/1532-429X-15-92
34. Kellman P, Wilson JR, Xue H, Ugander M, Arai AE. Extracellular volume fraction mapping in the myocardium, part 1: evaluation of an automated method. *J Cardiovasc Magn Reson*. 2012;14:63–74. doi: 10.1186/1532-429X-14-63
35. Safdar Z. Circulating collagen indices indicative of disease severity in pulmonary arterial hypertension. *Eur Respir J*. 2012;40:P2735.
36. Meissburger B, Stachorski L, Röder E, Rudofsky G, Wolfrum C. Tissue inhibitor of matrix metalloproteinase 1 (TIMP1) controls adipogenesis in obesity in mice and in humans. *Diabetologia*. 2011;54:1468–1479. doi: 10.1007/s00125-011-2093-9
37. Dziadzio M, Smith RE, Abraham DJ, Black CM, Denton CP. Circulating levels of active transforming growth factor beta1 are reduced in diffuse cutaneous systemic sclerosis and correlate inversely with the modified Rodnan skin score. *Rheumatol (Oxford)*. 2005;44:1518–1524. doi: 10.1093/rheumatology/kei088
38. Karapanagiotidis GT, Antonitsis P, Charokopos N, Foroulis CN, Anastasiadis K, Rouska E, Argiriadou H, Rammos K, Papakonstantinou C. Serum levels of matrix metalloproteinases -1,-2,-3 and -9 in thoracic aortic diseases and acute myocardial ischemia. *J Cardiothorac Surg*. 2009;4:59–65. doi: 10.1186/1749-8090-4-59
39. Andersen S, Nielsen-Kudsk JE, Vonk Noordegraaf A, de Man FS. Right ventricular fibrosis. *Circulation*. 2019;139:269–285. doi: 10.1161/CIRCULATIONAHA.118.035326
40. Swift AJ, Rajaram S, Capener D, Elliot C, Condliffe R, Wild JM, Kiely DG. LGE patterns in pulmonary hypertension do not impact overall mortality. *JACC Cardiovasc Imaging*. 2014;7:1209–1217. doi: 10.1016/j.jcmg.2014.08.014
41. Sato T, Tsujino I, Ohira H, Oyama-Manabe N, Ito YM, Noguchi T, Yamada A, Ikeda D, Watanabe T, Nishimura M. Paradoxical interventricular septal motion as a major determinant of late gadolinium enhancement in ventricular insertion points in pulmonary hypertension. *PLoS One*. 2013;8:e66724–e66731. doi: 10.1371/journal.pone.0066724
42. McCann GP, Beek AM, Vonk-Noordegraaf A, van Rossum AC. Delayed contrast-enhanced magnetic resonance imaging in pulmonary arterial hypertension. *Circulation*. 2005;112:e268. doi: 10.1161/CIRCULATIONAHA.104.512848
43. Sanz J, Dellegrottaglie S, Kariisa M, Sulica R, Poon M, O'Donnell TP, Mehta D, Fuster V, Rajagopalan S. Prevalence and correlates of septal delayed contrast enhancement in patients with pulmonary hypertension. *Am J Cardiol*. 2007;100:731–735. doi: 10.1016/j.amjcard.2007.03.094